

## Supporting Information.

### 1 Steady-state and TCSPC emission data of 5CN8 in water at 333-nm excitation

#### 1.1 High pH experiments

The steady-state emission spectra collected at 333-nm excitation of 5CN8 at high pH (Fig. S1, left) have different spectral shapes than those observed at 280-nm excitation (Fig. 1 in main text). The difference was attributed to large differences in the absorption by the neutral and anionic species at 280 nm vs. 333 nm (Table S1) and a higher emission yield by the neutral species upon excitation. For reference, the mole fractions of the different protic species are shown in Fig. S2. Indeed, the normalized emission spectra at 280-nm and 333-nm excitation could be overlaid at pH = 4.2 and pH 11.9 as only the neutral or anionic species, were present, respectively, in the ground state (Fig. S1, right). In contrast, the pH = 9.0 emission spectra could not be overlaid, as the pH was near the  $pK_a$  and both the neutral and anionic species are present. For the 333-nm excitation data, the neutral and anion have similar absorptivity, but the excited neutral species has a higher emission yield; hence, the emission peak appears to barely shift from the neutral emission peak. The TCSPC emission decay at 435 nm at 333-nm excitation, however, could still be fit to a biexponential equation with lifetimes identical to those observed in the 280-nm excitation (Fig. S3).

**Table S1.** Comparison of the absorbances of the different 5CN8 protic species at 280 nm and 333 nm within a pH titration measurement.

	Abs (280-nm)	Abs (333-nm)
<b>Cation</b>	0.19	0.17
<b>Neutral</b>	0.10	0.37
<b>Anion</b>	0.73	0.29

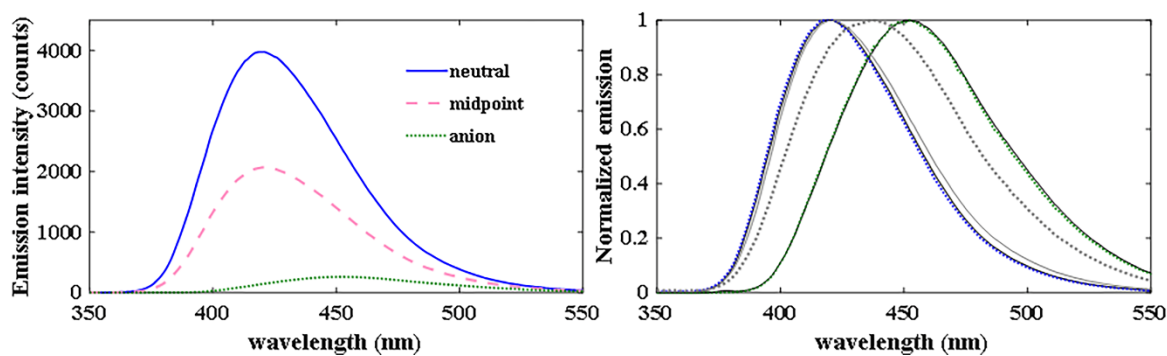
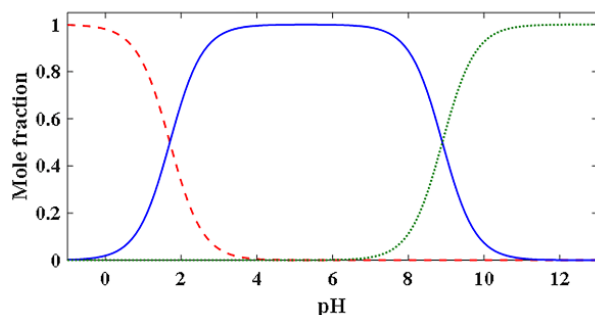


**Figure S1.** *Left:* Steady-state emission spectra of 5CN8 at 333-nm excitation under high pH conditions: neutral (pH = 4.2, solid blue line) and anion (pH 11.9, dotted green line). The emission near the ground state  $pK(OH)$  (pH = 9.0, dashed pink line) is shown for reference. *Right:* Normalized emission spectra of 5CN8 at pH = 4.2 and pH = 11.9 at 280-nm (blue and green dashed lines) and 333-nm excitation (solid black lines). The pH = 9 spectra at 280-nm (dashed) and 333-nm (solid) lines are also shown in grey.



**Figures S2.** Calculated mole fractions of the cationic (red dashed line), neutral (blue solid line), and anionic (green dotted line) species of 5CN8 based on  $pK_{a1} = 1.7$  and  $pK_{a2} = 8.9$  for a diprotic acid.

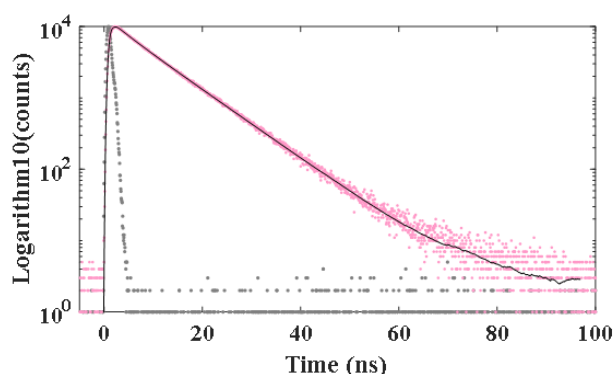


**Figure S3.** TCSPC emission decay and fit of 5CN8 at 333-nm excitation: pH =9.1 at 435 nm:  $\tau_1 = 9.0$  ns,  $\tau_2 = 3.45$  ns with weights  $\alpha_1 = 0.13$  and  $\alpha_2 = 0.87$ ,  $\chi^2 = 1.19$  (pink data, black solid line fit). The prompt is shown in grey.

## 1.2 Low pH experiments

Steady-state emission spectroscopy was much more sensitive to the presence of the neutral species in the ground state than absorption spectroscopy; hence, comparison of the 280-nm and 333-nm emission data served as an excellent control for the low pH studies, as the spectra would only overlap when the cationic species was completely isolated in the ground state. At pH=2, there is still a significant fraction of neutral species present in the ground state (see Fig. S2). 333-nm excitation preferentially excites the neutral species, while the 280-nm excitation preferentially excites the cationic species; however, as the neutral quantum yield is higher than the cationic species, the neutral emission peak dominates for both spectra and hence the two almost overlap (Fig. S4 A). Note, however, that the zwitterion tail resulting from the cation excitation is stronger in the 280-nm excitation spectrum. At pH=0, while the cation dominates, there is a minute fraction of neutral present; hence the two spectra do not overlap (Fig. S4 B). At pH = -0.5 and -1, the cation is nearly isolated in the ground state, and the 280-nm and 333-nm excitation data start to overlap (Fig. S4 C and D). Complementary TCSPC emission data were collected at the lowest pH; however, the emission decays were too fast to be studied with our instrumentation (Fig. S5).

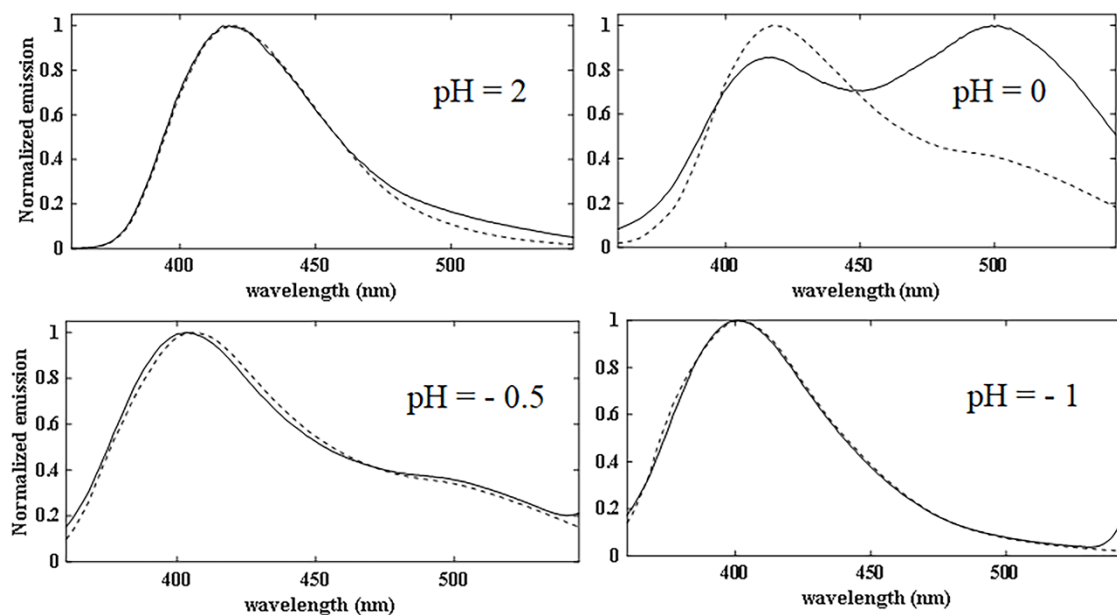


**Figure S4.** Comparison of the steady-state emission spectra of 5CN8 collected at 280-nm (solid line) vs. 333-nm (dashed line) excitation: *Top row:* A) pH = 2, B) pH = 0 *Bottom row:* C) pH = -0.5 and D) pH = -1.

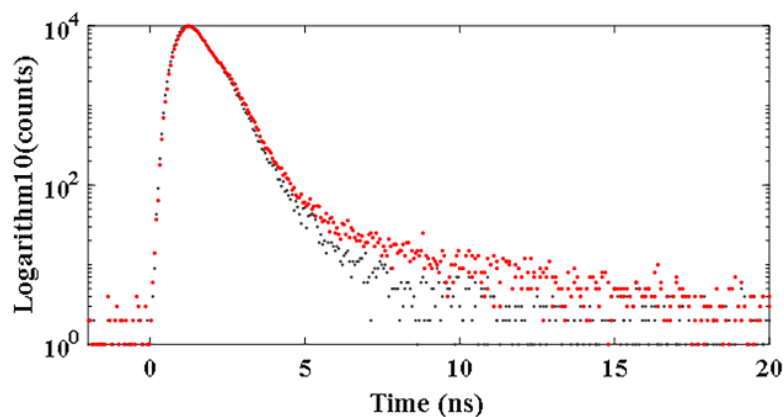


**Figure S5.** TCSPC emission decay at 410 nm of 5CN8 at 280-nm excitation. The pH = -1 data is shown in red, while the instrument prompt is shown in grey.

## 2 Spectral data of 5CN8 in methanol

A comparison of the absorption spectra of the cationic and neutral species of 5CN8 in methanol vs. water is shown in Fig. S6. The spectral features are redshifted in methanol but have similar shapes. The steady-state and TCSPC emission data for the neutral species are also provided below (Fig. S7), while information about the cationic species is provided in the main text. Compared to water, the emission peak for the neutral species blueshifts ( $\sim 409$  nm vs. 419 nm in water) and has a shorter lifetime:  $\tau = 5.6$  ns vs. 9.1 ns in water.

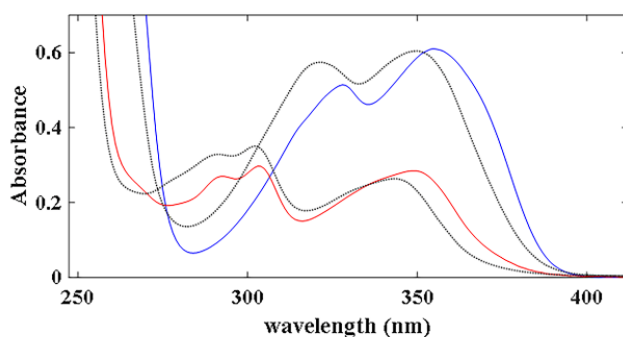


**Figure S6.** Comparison of the absorption spectra of 5CN8 in methanol vs. water: the solid blue and red lines correspond to the neutral and cationic species, while the dotted lines were collected in water.

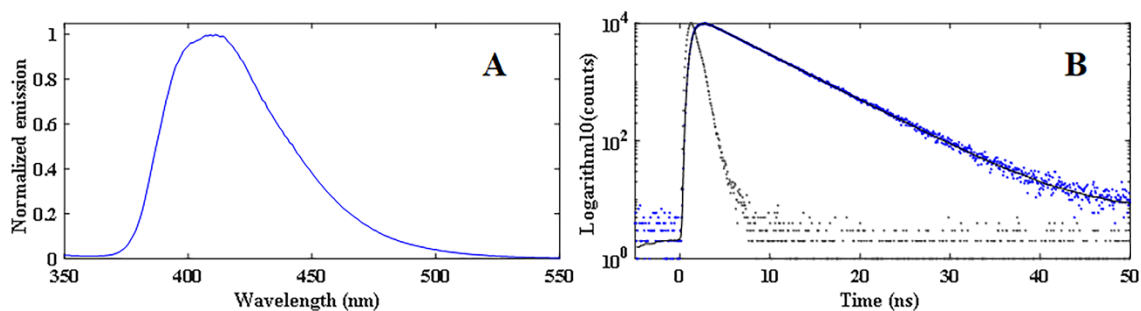


**Figure S7.** A. Steady-emission spectrum of neutral 5CN8 in methanol; B. TCSPC emission decay of neutral species at 420 nm with fit:  $\tau = 5.6$  ns,  $\chi^2 = 1.12$  (blue data, black solid line fit). The instrument prompt is shown in grey.

### 3 Computational SI

#### 3.1 CO and CN bond lengths of interest

**Table S2.** The calculated CO bond lengths for the ground and excited acid undergoing ESPT at the OH site using B3LYP/6-311++G(d,p) and TD-DFT. In grey are the values associated with 55CN8.

Proton donor	pK <sub>a</sub> <sup>*</sup> (OH)	CO (Å) of S <sub>1</sub> /S <sub>0</sub> acid
5CN2OH	-0.75	1.33998 / 1.36716
55CN8 cation	-0.3	1.33303 / 1.35822
8N2OH cation	1.1	1.34127 / 1.36276
2OH	2.8	1.35104 / 1.37126
55CN8 neutral	(8.9)	1.36305 / 1.36861
8N2OH neutral	(9.5)	1.37364 / 1.37251

**Table S3.** The calculated CN bond lengths for the ground and excited acid and conjugate base undergoing ESPT at the NH<sub>3</sub><sup>+</sup> site using B3LYP/6-311++G(d,p) and TD-DFT. In grey are the values associated with 55CN8.

Proton donor	pK <sub>a</sub> <sup>*</sup> (NH <sub>3</sub> <sup>+</sup> )	CN (Å) of S <sub>1</sub> /S acid	CN (Å) of S <sub>1</sub> /S <sub>0</sub> conjugate base
1N	-1.1	1.47188 / 1.48167	1.35291 / 1.39835
55CN8 cation	-0.3	1.47281 / 1.47924	1.35648 / 1.37787
8N2OH cation	(4)	1.47336 / 1.48097	1.35441 / 1.40219

#### 3.2 HOMA analysis of 2OH

The aromaticity of the carbon rings of excited 2OH (Fig. S8) and its conjugate base were evaluated using HOMA analysis:

$$HOMA = 1 - \frac{\alpha_j}{n} \sum_i^n (R_{opt,j} - R_{j,i})^2$$

with  $R_{opt} = 1.388$  and  $\alpha = 257.7$  for CC bonds.<sup>1</sup> In this analysis, only the CASSCF calculations showed an increase in aromaticity (or relief in the antiaromaticity) upon excitation (Table S4, bold). For comparison, HOMA calculations were repeated with inclusion of the CO bond,  $R_{opt} = 1.265$  and  $\alpha = 157.38$ .<sup>1</sup> The B3LYP calculations showed an increase in aromaticity; however, the WB97XD calculations still did not, illustrating the difficulty of using TD-DFT methods to predict photoacidity via aromaticity/antiaromaticity factors in naphthol compounds. The calculated  $\Delta HOMA$  for the B3LYP calculations was also smaller than that predicted by CASSCF.

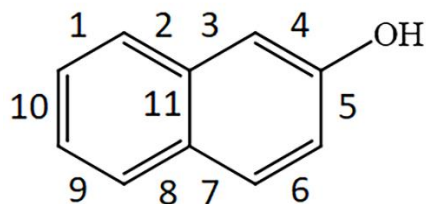


**Figure S8.** Picture of 2OH with CC bonds labeled 1-11 for the HOMO analysis.

**Table S4.** The calculated CC bond lengths (Å) of the excited 2OH acid/conjugate base using different levels of computational theory are listed. The numbering of the CC bonds corresponds to Fig. S8. The HOMA results for each species are provided below, with and without the inclusion of the CO bond. In bold are cases in which the excited 2OH conjugate base had a higher calculated aromaticity than the acid.

Bond length	B3LYP	WB97XD	CASSCF <sup>a</sup>
CC1	1.42578 / 1.42525	1.41980 / 1.41540	1.41014 / 1.43328
CC2	1.41761 / 1.41646	1.41241 / 1.41337	1.41033 / 1.39923
CC3	1.41293 / 1.42014	1.40351 / 1.40553	1.40920 / 1.42194
CC4	1.43632 / 1.44693	1.43773 / 1.45889	1.40857 / 1.44210
CC5	1.39167 / 1.44028	1.38568 / 1.43430	1.41762 / 1.44850
CC6	1.41686 / 1.39760	1.41266 / 1.39639	1.40978 / 1.38897
CC7	1.42321 / 1.42682	1.41837 / 1.42589	1.41018 / 1.41925
CC8	1.41265 / 1.43078	1.40376 / 1.41566	1.41129 / 1.43129
CC9	1.42952 / 1.41333	1.42568 / 1.41086	1.41078 / 1.41233
CC10	1.38509 / 1.39544	1.38146 / 1.39247	1.42209 / 1.39107
CC11	1.45005 / 1.44847	1.45275 / 1.45399	1.49951 / 1.44813
CO	1.35098 / 1.28184	1.34077 / 1.26654	1.34953 / 1.24704
<b>HOMA</b>	0.68287 / 0.59660	0.72449 / 0.62424	<b>0.56981 / 0.60211</b>
<b>HOMA (CO)</b>	<b>0.61235 / 0.62650</b>	0.67216 / 0.65553	<b>0.51194 / 0.63104</b>

#### Reference for Computational Supplementary Information

1. T. M. Krygowski, *J Chem Inf Comput Sci*, 1993, **33**, 70-78.